

Thermophotovoltaic Cells Based on Low-Bandgap Compounds

V.P.Khvostikov, V.D.Rumyantsev, O.A.Khvostikova, M.Z.Shvarts
P.Y.Gazaryan, S.V.Sorokina, N.A.Kaluzhniy, V.M.Andreev

Ioffe Physico-Technical Institute, 26 Polytechnicheskaya, St.Petersburg, 194021, Russia

Abstract. High efficiency TPV GaSb and Ge based cells fabricated by a non-toxic and inexpensive Zn-diffusion technique have been developed. GaSb based cells optimised for operation with solar powered photon emitter allowed increasing the efficiencies up to 27-28% at black body temperature > 2000 K assuming 90% reflection of sub-bandgap photons. Combination of the MOCVD technique or LPE growth and Zn diffusion from the gas phase allows fabricating Ge photocells on the base of the GaAs/Ge heterostructures, which are characterized by high photocurrent and open circuit voltage values. Efficiencies of 13% were obtained in GaAs/Ge TPV cells under the black-body (1700-2100 K) irradiation assuming the achieved 90% reflection of sub-bandgap photons.

INTRODUCTION

Sunlight is an ecologically safety and available energy source with a high energetic potential. Employment of concentrated sunlight as a heat source in a TPV system [1-4] is promising for increase in TPV conversion efficiency with retention of all advantages of sunlight converters. The use of hybrid solar-fuel systems may allow operating a TPV generator 24 hours a day: at night – a thermal TPV and in the daytime – a solar powered TPV (STPV) system [5, 6] with a sunlight concentrator.

In a TPV system there are certain possibilities to improve the efficiency. One of the ways of gaining in the TPV generator efficiency is associated with the use of the energy of the “useless” long-wavelength radiation to make higher the emitter temperature. The low-energy photon recirculation effect can be achieved by introduction of a reflector on the cell back side, for example, by depositing a dielectric cover and a metal film on the back wafer surface.

This paper describes the features of the developed GaSb and Ge cells for TPV applications. In particular, it is shown on the bases of measured photovoltaic parameters of the cells (spectral response, quantum efficiency, open circuit voltage, fill factor) and calculated spectra of the black-body-type photon emitters, that efficiencies as high as 30% can be achieved in a solar powered TPV system with a concentration ratio of about 10^4 suns, and receiver/emitter photon recycling efficiency of 90%.

GaSb BASED TPV CELLS

The following features of the GaSb cells have been under investigation at the presented stage of work:

- reflection coefficient of the sub-bandgap photons for the samples with different doping levels and thicknesses;
- quality evaluation of the GaSb ingots and wafers;
- evaluation of the Zn profiles after diffusion process;
- estimation of the TPV conversion efficiencies in practical cells.

Reflection Coefficient For Sub-Bandgap Photons

It had been pointed out that the TPV system efficiency depends to large extent on effective employment of sub-bandgap photons. We have investigated the dependences of the “useless” infrared radiation reflection coefficient for GaSb samples on their free carrier concentration and thickness.

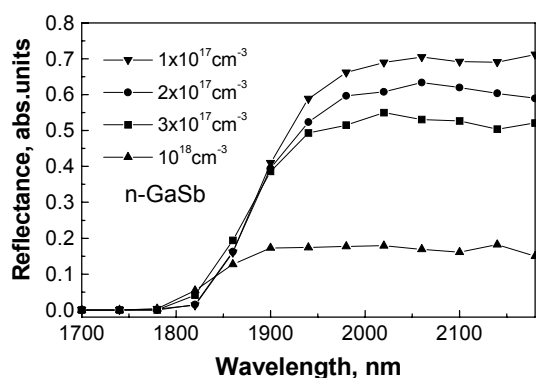


FIGURE 1. Reflectance of the Te-doped n-GaSb samples (450 μm thick) with different doping levels. The samples have the front ZnS/MgF₂ ARC coating and MgF₂/Au back-surface mirror.

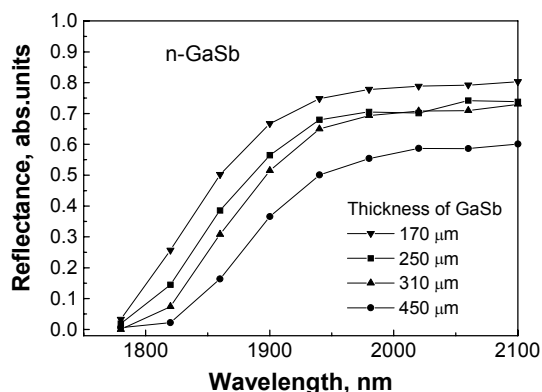


FIGURE 2. Reflectance of the GaSb samples ($n = 2 \times 10^{17} \text{ cm}^{-3}$) with different thicknesses. The samples have front ZnS/MgF₂ ARC coating and the MgF₂/Au back-surface mirror.

In the developed GaSb cells, the back-surface mirror consists of MgF₂ and Au layers [7]. All samples have ZnS/MgF₂ ARC coating. Figures 1 and 2 show spectral dependences of reflectance on free carrier concentration and wafer thickness. Figure 3 presents reflectance versus carrier concentration and wafer thickness for GaSb samples at wavelength $\lambda = 2100 \text{ nm}$. As it is seen from these figures maximum reflectance of 80% at wavelengths longer than 2.0 μm may be obtained for GaSb cells (170 μm thick $n = 2 \times 10^{17} \text{ cm}^{-3}$).

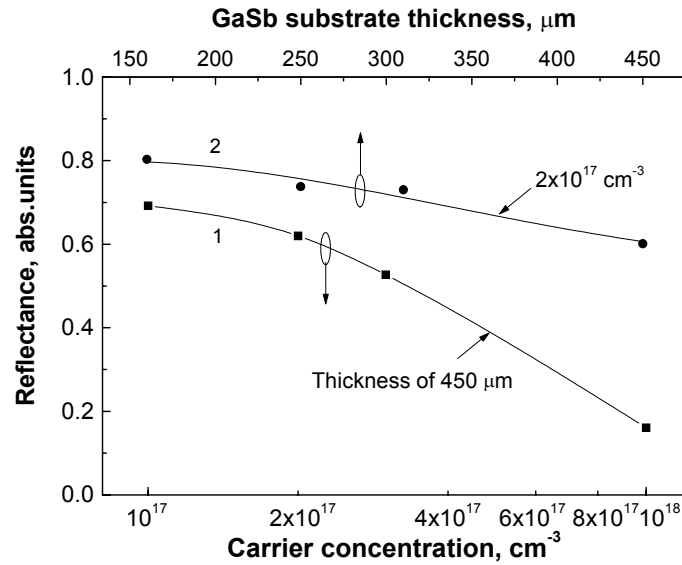


FIGURE 3. Reflectance of n-GaSb samples vs carrier concentration (450 μm thick - curve 1) and thickness ($n = 2 \times 10^{17} \text{ cm}^{-3}$ - curve 2) at wavelength $\lambda = 2100 \text{ nm}$.

Quality Evaluation Of GaSb Ingots And Wafers

For GaSb TPV cells a good quality bulk semiconductor material is required to produce high efficient PV converters by Zn diffusion process [7-9].

It has been found (see in Fig. 4, 5) that GaSb ingots grown by the Czochralski technique and doped with tellurium have inhomogeneities due to gradual variation of doping impurity concentration and electron mobility along an ingot. It is seen from the Hall measurements at 77 K, that carrier mobility increases along the ingot in 1.5 - 2 times, whereas for electrically active impurity concentration it is 5 - 10 times higher.

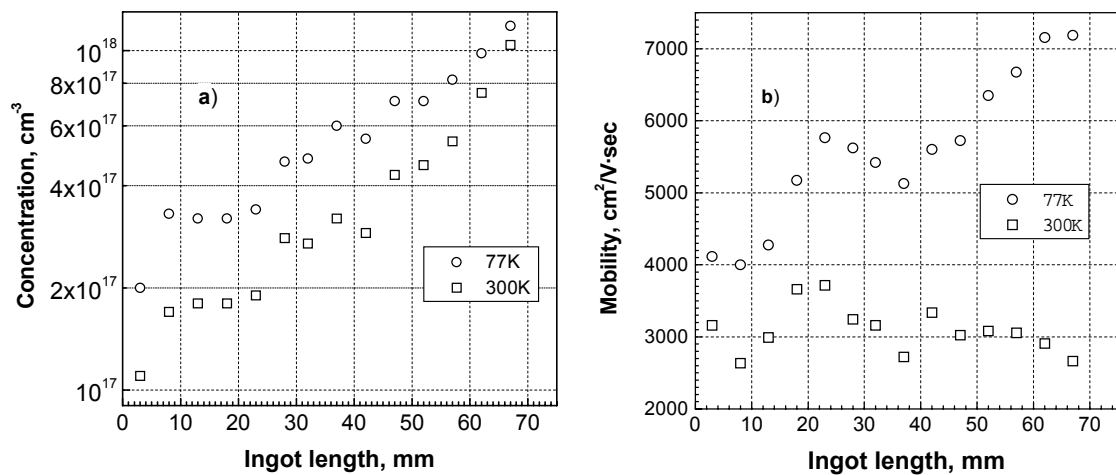


FIGURE 4. Hall measurements of free carrier concentration (a) and mobility (b) along GaSb ingot N96.

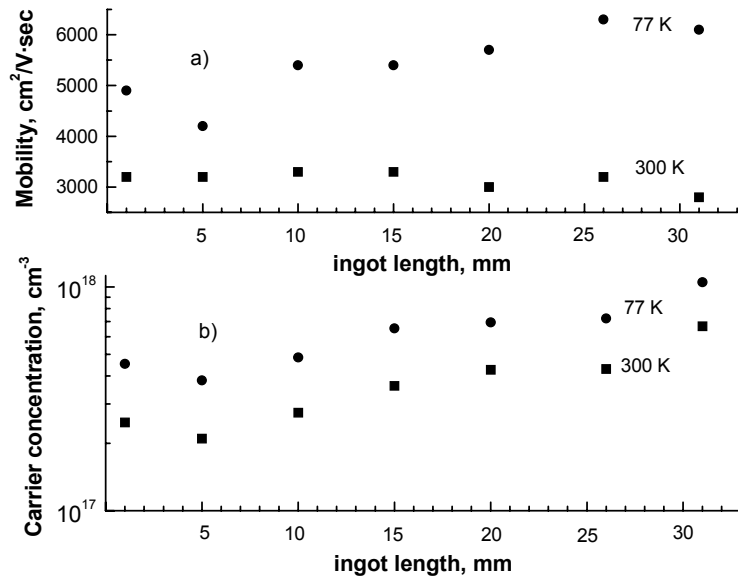


FIGURE 5. Hall measurements of free carrier mobility (a) and concentration (b) along GaSb ingot N93.

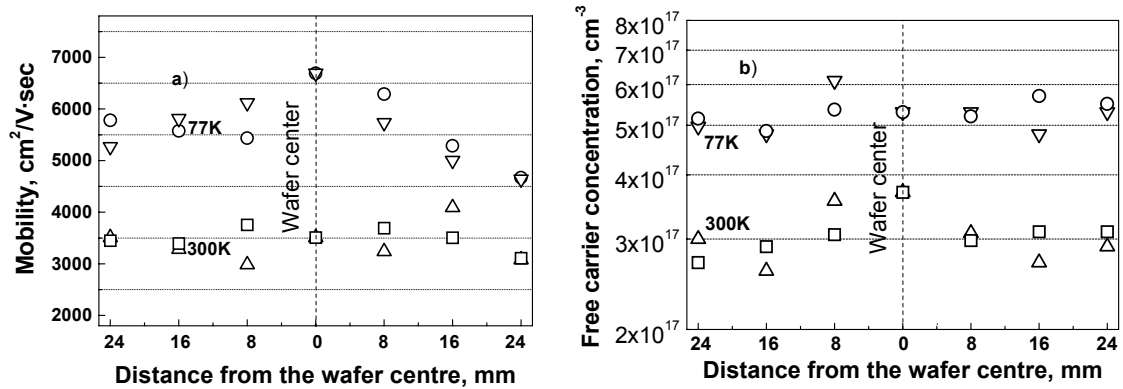


FIGURE 6. Hall measurements of carrier mobility (a) and concentration (b) for GaSb (Te) wafer N36 from ingot N93 in two perpendicular directions.

The concentration gradient of the electrically active impurities along the ingot is, apparently, associated with the rise of Te concentration resulted from enriching the melt with Te during growth period. The carrier mobility value may serve as a measure of existence of additional impurity formations and defects. The mobility in the ingots under investigation increases to the ingot end. Its rise, in spite of the tellurium concentration increase, may be explained, for example, by the uncontrolled impurity content and by formation of clusters in the crystal. The transverse inhomogeneity of the ingot (Fig. 6) resulted from the Te concentration and carrier mobility variations by 20-30% in the radial direction. The above inhomogeneity values may partly be explained by errors of the Hall measurements, and in total can not influence the main characteristics of TPV cells fabricated with this wafers.

Thus, near to 80% of the GaSb ingot may be used for fabrication of wafers for high efficiency TPV cells, but without taking into account the reflection of sub-bandgap photons. And only 30-50% of the GaSb ingot can be considered as the most suitable for achievement of maximum reflection in GaSb based TPV cells.

Evaluation Of The Zn Profiles

TPV cells are fabricated by a relatively simple method of zinc diffusion from the gas phase at relatively low temperatures (470-490 °C) in a pseudo-closed box in the hydrogen flow. An increase in the exposure time up to 1 hour allowed us to form *p-n* junctions laying in the depth of 0.4 - 0.6 μm. One of the ways to simplify the technological cycle of formation of an optimum *p-n* junction relief is Zn diffusion through semipermeable films deposited on the wafer surface with spacial selection. In this case the base active layer and under-contact regions can be formed during one-stage diffusion process.

In the present work we have used the thin layers of the anodic oxide on the GaSb surface as a special semipermeable mask at Zn diffusion. Our experiments have shown, that, instead of expected braking of the mass transport, anodic oxidation of the wafer resulted in essential acceleration of Zn diffusion into bulk GaSb. For example, zinc diffusion from the gas phase through anodic oxide film 0.16 μm thick (it was formed at the voltage of 80 V) allowed increasing in both *p-n* junction depth (almost in two times compared to the diffusion into the samples without oxidation) and surface impurity concentration (in 1.5 – 2 orders of magnitude). Corresponding profiles of Zn distribution measured by SIMS method are shown in Fig. 7.

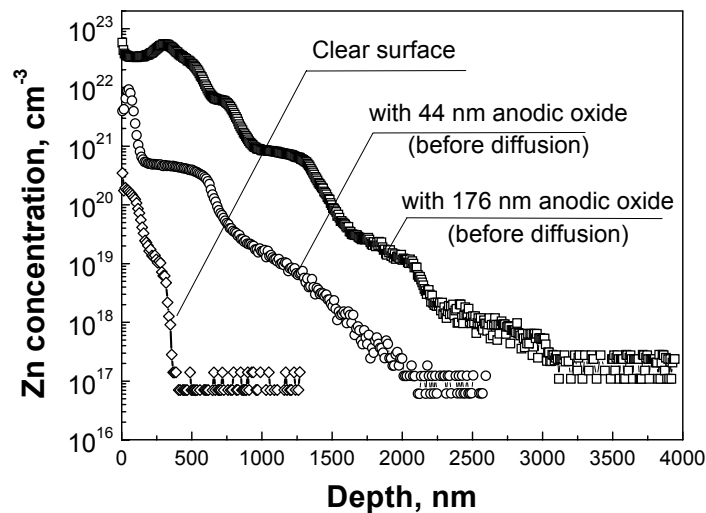


FIGURE 7. Free carrier distribution profiles at Zn diffusion into GaSb wafers from the gas phase in the case of clear and oxidized sample surfaces before diffusion.

Therefore, anodic oxide assists the intensive Zn absorptions from the gas phase. Anodic oxide may be used for local increase in depth of the diffused *p-n* junction in

the places intended for contact grid deposition. Being characterized by improved chemical stability after thermal treatment such films are not removed from the GaSb surface.

Introduction of a subcontact layer of anodic oxide after its thermal treatment allows improving contact metal adhesion and even reducing contact resistance.

Estimation Of The TPV Conversion Efficiency

Back-surface reflection of non-absorbed sub-bandgap photons in a TPV cell allows maximizing the efficiency of a STPV system owing to possible reabsorption of these photons in the emitter. GaSb TPV cell photocurrent densities and efficiencies have been calculated on the basis of measured parameters, such as fill factor, open circuit voltage and photosensitivity spectrum curve of the practical cells developed in the PV Lab of the Ioffe Institute. Corresponding data are plotted in Fig. 8 as the function of a black body IR-emitter temperature for different reflectance values for sub-bandgap photons.

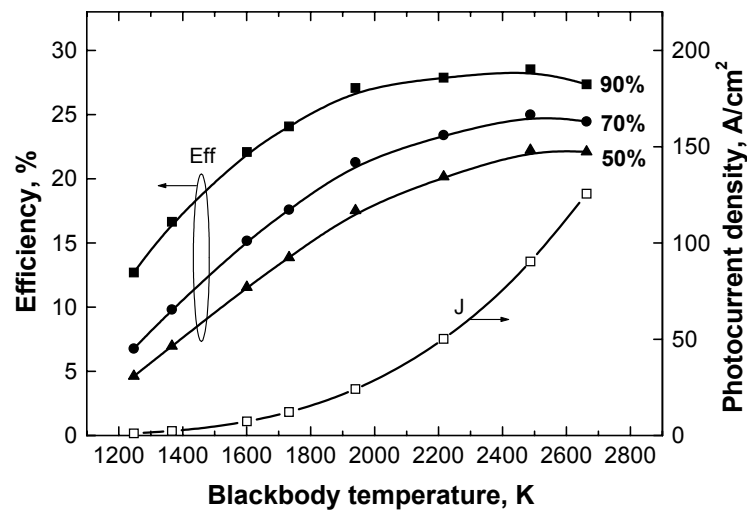


FIGURE 8. GaSb TPV cell photocurrent densities and efficiencies versus black body IR-emitter temperature. Reasonable cell-emitter reflectance values of 50%, 70%, and 90% for sub-bandgap photons are assumed.

Efficiencies as high as 27-28% are predicted in these cells for the case of 90% return efficiency and $T_{BB} > 2000$ K.

Ge BASED TPV CELLS

TPV cells based on GaAs(thin window)/Ge heterostructures have been fabricated by using two approaches. The first of them was combination of metal-organic chemical-vapor deposition of GaAs layer and Zn diffusion from the gas phase. Fabrication procedure included deposition of a Si_3N_4 dielectric coating, opening the windows in it, and selective diffusion of Zn. Such an approach resulted in a comparatively high

photocurrent density and open-circuit voltage in the cells, what can be explained by planar growth of a wide-gap GaAs window as thin as 0.1 μm and by the fact that the $p-n$ junction does not extend to the opened surface of the cell. In the measurements the open-circuit voltage increased linearly with the photocurrent density up to 0.42–0.43 V at photocurrent density of 10 A/cm². To our knowledge, this is the maximum open-circuit voltage for such Ge based cells measured under similar conditions. Conversion efficiency, being calculated for one-sun photocurrent density of 28.9 mA/cm² AM0 spectrum reaches its maximum of 5.5–5.7% at 200-fold sunlight concentration [10].

The second approach was the following. The p-GaAs/p-Ge/n-Ge heterostructures with a thin (0.1 μm) GaAs layer were grown by low-temperature (380 °C) liquid-phase epitaxy. Additional Zn-diffusion process into the p-GaAs-n-Ge heterostructure was necessary in this case. The advantage of this technology compared to MOCVD is avoiding the undesirable diffusion of Ga and As atoms from vapour phase into Ge owing to much lower growth temperature in LPE process.

Reflectance measurements for Ge samples with different types of back surface mirrors and different doping levels of bulk material have been carried out. The results are presented in Fig. 9, 10. Reflectance above 90% has been achieved in Ge samples 300 μm thick with doping level $n = 10^{17} \text{ cm}^{-3}$.

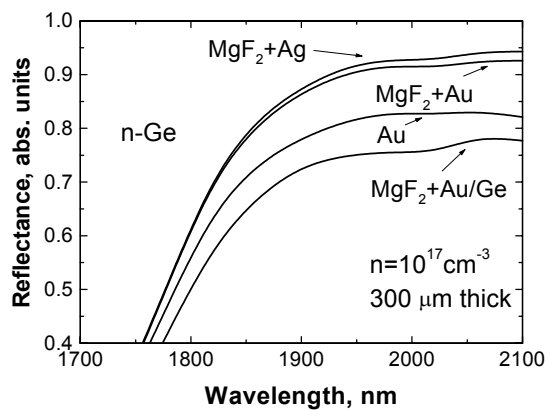


FIGURE 9. Reflectance vs. wavelength for n-Ge samples with different back surface mirrors. The samples have front ZnS/MgF₂ ARC coating.

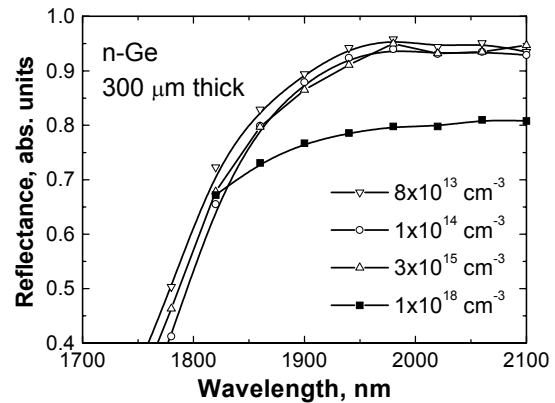


FIGURE 10. Reflectance vs. wavelength for n-Ge samples with different doping levels. Samples have ZnS/MgF₂ ARC coating and MgF₂/Au back surface mirror.

Figure 11 demonstrates dependences of LPE grown GaAs/Ge TPV cell efficiencies, calculated on the basis of practically measured photovoltaic parameters in the same way, as it was done for GaSb cells. Efficiency of 16% is predicted in these cells under black-body irradiation (1700-2100 K) assuming 100% reflectance for sub-bandgap photons.

Comparison of the results presented in Fig. 8 and Fig. 11 shows that efficiencies in Ge cells are lower than in GaSb cells. However, the developed GaAs/Ge cells have prospects for application in solar TPV systems taking into account the lower price of

Ge wafers and possibility to obtain a higher reflectance (Fig. 9, 10) for these cells in comparison with GaSb cells (Fig. 1-3).

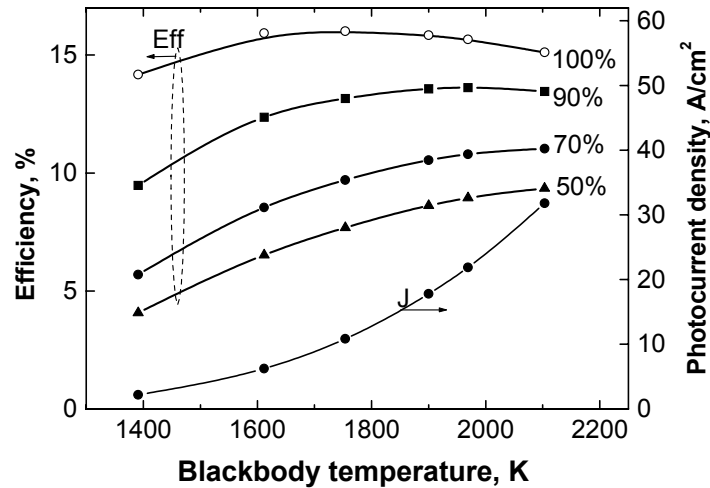


FIGURE 11. LPE grown GaAs/Ge TPV cell efficiencies as a function of a black-body emitter temperature. Reasonable cell-emitter reflectance values of 50%, 70%, 90% and 100% reflection of sub-bandgap photons from the cell to the emitter is assumed.

CONCLUSIONS

Reflectance measurements for GaSb and Ge based samples with different types of back surface mirrors in dependence on bulk doping level (GaSb, Ge) and thickness (GaSb) have been carried out. Maximum measured reflectance is about 80% for the GaSb samples 170 μm thick with the doping level of $2 \times 10^{17} \text{ cm}^{-3}$. More than 90% reflectance has been achieved for Ge samples 300 μm thick with free carrier concentration of 10^{17} cm^{-3} .

The TPV efficiencies of 27-28% have been achieved in GaSb cells fabricated by the optimised Zn diffusion method. Cell efficiencies have been calculated on the basis of PV parameters measured in practical cells. Similar calculations for developed Ge based cells with GaAs window layer gave lower efficiencies (no more, than 16%).

ACKNOWLEDGEMENTS

The authors wish to thank Zh.Alferov and A.Luque for helpful discussions and to express our gratitude to N.H.Timoshina and A.I.Dement'eva for their contribution to this work.

This work has been supported by the European Commission through the funding of the project FULLSPECTRUM (Ref. N: SES6-2003-502620).

REFERENCES

1. P. A. Davies, A. Luque, "Solar thermophotovoltaics: Brief review and a new look", *Solar Energy Materials & Solar Cells*, **33**, 11-22 (1994).
2. V. Badescu, "Thermodynamic theory of thermophotovoltaic solar energy conversion", *J. Appl. Phys.*, **90**, 6476-6486 (2001).
3. K. W. Stone, N. S. Fatemi, L. Garverick, "Operation and component testing of a solar thermophotovoltaic power system", *Proc. of 25th IEEE PVSC*, Washington, DC, 1996, 1421-1424.
4. H. Yugami, H. Sai, K. Nakamura, N. Nakagama, H. Ohtsubo, "Solar thermophotovoltaic using $\text{Al}_2\text{O}_3/\text{Er}_3\text{Al}_5\text{O}_{12}$ eutectic composite selective emitter" *Proc. 28th IEEE PVSC*, Anchorage, 2000, pp. 1214-1217.
5. V. D. Romyantsev, V. P. Khvostikov, O. A. Khvostikova, P. Y. Gazaryan, N. A. Sadchikov, A. S. Vlasov, E. A. Ionova, V. M. Andreev "Structural Features of a Solar TPV Systems", *6th Conference on Thermophotovoltaic Generation of Electricity*, Freiburg, 2004 (in this book).
6. V. M. Andreev, V. P. Khvostikov, O. A. Khvostikova, V. D. Romyantsev, P. Y. Gazaryan, A. S. Vlasov, "Solar Thermophotovoltaic Converters: Efficiency Potentialities", *6th Conference on Thermophotovoltaic Generation of Electricity*, Freiburg, 2004 (in this book).
7. V. M. Andreev, V. P. Khvostikov, O. A. Khvostikova, E. V. Oliva, V. D. Romyantsev, M. Z. Shvarts, "Thermophotovoltaic Cells with Sub-bandgap Photon Recirculation", *Proc. of 17th European Photovoltaic Solar Energy Conf.*, Munich, 2001, pp. 219-222.
8. A. W. Bett, S. Keser, O. V. Sulima "Study of Zn Diffusion into GaSb from the Vapour and Liquid Phase", *J. of Crystal Growth* **181**, pp. 9-16 (1997).
9. G. Stollwerck, O. V. Sulima, A. W. Bett, "Characterization and Simulation of GaSb Device-Related Properties", *IEEE Transactions on Electron Devices* **47** (2), pp. 448-457 (2000).
10. V. Andreev, V. Khvostikov, O. Khvostikova, N. Kaluzhniy, E. Oliva, V. Romyantsev, S. Titkov, M. Shvarts, "Low-Bandgap PV and Thermophotovoltaic Cells", *3rd World Conference on Photovoltaic Energy Conversion*, Osaka (2003).